

# Firing, quenching and annealing studies on thick-film resistors

S. Vionnet<sup>1</sup>, Th. Maeder<sup>1,2</sup>, P. Ryser<sup>1</sup>

1) Laboratoire de Production Microtechnique, EPFL, CH-1015 Lausanne, Switzerland.

2) Sensile Technologies, PSE, CH-1015 Lausanne, Switzerland

**Version of record:** Journal of the European Ceramic Society 24 (6), 1889-1892, 2004.

[http://hdl.handle.net/10.1016/S0955-2219\(03\)00462-X](http://hdl.handle.net/10.1016/S0955-2219(03)00462-X)

## Abstract

In this work, we aim to understand the firing behaviour of three representative thick-film resistor compositions used in force and pressure sensors. The dependence of the materials' microstructure and properties (sheet resistance and its temperature coefficient, gauge factor) is studied as a function of firing temperature and time, and cooling rate (furnace or quench). The stability of the properties is assessed by annealing at intermediate temperatures (100 and 250°C). Microscopic and structural analysis is also carried out. The results are discussed in the light of the possible evolution mechanisms of the resistor materials: diffusion, dissolution, precipitation and stress relaxation.

**Keywords:** *Electrical properties; Firing; Quenching; Sensor; Thermal properties*

## 1 Introduction

Due to their good stability and piezoresistive response, thick-film resistors (TFR) have found wide application in the field of pressure and force sensors. TFR pastes consist basically of a fine-grained (20-100 nm) conductive phase (RuO<sub>2</sub> or ruthenate), a lead borosilicate glass frit (1-3 µm) and an organic vehicle<sup>1</sup>. Some other oxides are also added as minor additives to modify the temperature coefficient of resistance (*TCR*) or the temperature coefficient of expansion (*TCE*) of the glass phase<sup>2</sup>. Upon firing, the organic material is first burned out, followed by densification of the material to give a nanoscale composite consisting of chains of conductive islands in an insulating matrix.

The ratio between conductive and glass phases roughly determines the specific resistivity of the resistor. During the firing cycle, the constituents of the materials react with each other (conductive oxides, glass phase and additives). Dissolution / reprecipitation of the conductive phase have been observed<sup>3</sup>. Also, the conductive phase may exchange PbO with the glass matrix, leading to decomposition of ruthenate into RuO<sub>2</sub> or the reverse reaction depending on the glass composition and firing temperature<sup>3</sup>. Reaction of the glass with the alumina substrate has also been observed<sup>4</sup>. The usual firing and cooling times (each ca.10 min) are presumably not sufficient for the material to reach equilibrium<sup>2</sup>, as increasing firing time, firing temperature or refiring several times lead to significant changes in structure, chemistry and electrical properties<sup>5,6,7</sup>.

This work aims to study the influence of the firing schedule (temperature, time and cooling rate) on the properties and stability of several TFR compositions. Studies by scanning electron microscopy (SEM), and X-ray diffraction (XRD) are also carried out.

## 2 Experimental

In this work, three compositions with  $R_s = 10$  kΩ/sq nominal sheet resistance were evaluated: 1) Du Pont (DP) 2041: a standard composition widely used in piezoresistive sensors, 2) Electro Science Laboratories (ESL) 3414: specifically formulated to have high gauge factor (*GF*) values and 3) ESL 3114: a low-firing (625 vs. 850°C for DP 2041 & ESL 3414) composition for applications on enamelled steel substrates. These compositions exhibit different conductive phases: RuO<sub>2</sub> only in ESL 3114, ruthenate (Bi<sub>2</sub>Ru<sub>2</sub>O<sub>7</sub>) only in ESL 3414, and a mixture of RuO<sub>2</sub> and ruthenate (presumably Pb<sub>2</sub>Ru<sub>2</sub>O<sub>6.5</sub>) in DP 2041<sup>2</sup>.

All the substrates were 96% pure alumina (Kyocera, Japan, A-476), the standard thick-film substrate material. In order to minimise termination effects, gold (ESL 8837) was chosen as termination material. A single layout was used to provide samples for all measurements: structural and microscopic investigations ( $10 \times 10 \text{ mm}^2$  squares),  $R_s$  and  $TCR$  (1.5 mm wide resistors of several lengths), and  $GF$  (Wheatstone bridge on cantilever beam),  $1 \times 1 \text{ mm}^2$  resistors.

Resistors of each composition were subjected to 7 different firing cycles: 1) “standard” resistor firing cycle, in a belt furnace, 10 min; 2/3) tube furnace, standard temperature, 1h, N/T; 4/5) tube furnace, standard temperature, 11h, N/T; 6/7) tube furnace, high temperature, 1h, N/T. “Standard” and “high” firing temperatures were 850 and 950°C for DP 2041 and ESL 3414, and 630 and 700°C for ESL 3114. Cooling times to 250°C were ca. 10 min (standard belt furnace), 5h (N, cooling in tube furnace), and 20 s (T, quenching by rapidly removing and exposing the samples to air). After firing, the samples were subjected to long-term annealing cycles at 100 and 250°C in order to ascertain their stability.

Measurements were performed after firing and ex situ during annealing, by periodically removing the samples from the annealing oven.  $R_s$  and  $TCR$  were measured as a function of resistor length between room temperature ( $RT = 23 \dots 26^\circ\text{C}$ ) and 100°C.  $R_s$  is always given at 25°C by correcting the RT value with the measured  $TCR$ .  $GF$  was determined at RT by suspending weights at the end of the test cantilevers, with test elastic strains of ca. 200 ppm. XRD spectra were realised with a Kristalloflex 805 Siemens diffractometer. SEM of the surface of the resistors were realised with Philips XL30 FEG microscope.

## 3 Results and discussion

### 3.1 Standard firing conditions

The initial (as-fired) properties of the resistors for the standard firing cycle (850°C, 10 min for DP 2041 and ESL 3414, and 630°C, 10min for ESL 3114) are given in Table 1. The negative  $TCR$  of ESL 3114 is expected due to the wide  $TCR$  tolerances for this paste and to the fact that it is adapted to steel substrates, which have a larger  $TCE$  than alumina.

The observed microstructures (Fig. 1) differ considerably: while DP 2041 has a fine microstructure, ESL 3114 and ESL 3414 exhibit a coarser segregation of conducting regions and glass-only areas. These observations are in accordance with previous work on DP 2041 and ESL 3414<sup>3</sup>.

### 3.2 Effect of firing schedule

The properties are given in Fig. 2 and 3 for the different firing schedules and the effect of each parameter (time, temperature, quenching) is given in table 2. No data is given for ESL 3414 fired at 950°C, as degradation at the terminations was found to occur; SEM observations show a 10  $\mu\text{m}$ -wide glassy area between electrode and resistor devoid of conductive particles. Except in this case, significant termination effects were not observed in this study, which is expected when using Au.

The effect of the firing schedule is quite different for each composition. Increasing firing thermal budget (temperature, time) causes a strong decrease of  $R_s$  for DP 2041, but a small decrease of  $GF$  values. ESL 3114 exhibits a much smaller corresponding  $R_s$  decrease, but a larger decrease of  $GF$ . Quenching DP 2041 affects significantly only its  $TCR$  (decreasing). On the other hand,  $R_s$  is strongly decreased for ESL 3414 (this will be subject of future investigations), and  $TCR$  increases for ESL 3114. Also, a small but significant increase of  $GF$  is observed for ESL 3414 and 3114.

Overfiring the resistors does not radically change the microstructure, but leads to coarsening of the conductive particles for all compositions, which implies diffusion of Ru in the glass<sup>8</sup>. XRD spectra show no apparent change for ESL 3114 (conductive phase:  $\text{RuO}_2$  only) and ESL 3414 ( $\text{Bi}_2\text{Ru}_2\text{O}_7$  only). In the case of DP 2041, progressive decomposition of  $\text{Pb}_2\text{Ru}_2\text{O}_{6.5}$  into  $\text{RuO}_2$  and  $\text{PbO}$  (the latter enters the glass) occurs, in accordance with the published stability data<sup>9</sup>. From XRD spectra, the mole fraction of Ru in ruthenate (vs. in  $\text{RuO}_2$ ) decreases from 64% (850°C, 10min) to 2% (950°C, 1h). The resulting  $\text{PbO}$  enrichment of the intergrain glass may contribute to the strong  $R_s$  decrease exhibited by DP 2041<sup>10</sup>. Also, firing DP 2041 at 950°C 1h precipitates a crystalline phase identified as  $\text{ZrSiO}_4$  by XRD<sup>2</sup>.

### 3.3 Post-annealing at 100°C and 250°C

No significant changes in properties are observed upon annealing at 100°C for all pastes. The maximum variation of  $R_s$  is  $< 0.08\%$ . Upon annealing at 250°C, similar results are obtained for  $GF$  and  $TCR$ . Also, no significant change of microstructure or XRD spectrum is observed.

However,  $R_s$  changes significantly at 250°C and its evolution, given as a function of annealing time in Fig. 4, is dependent on the firing schedule. No dependence on resistor length was observed, indicating absence of significant termination effects.

In general, stability for a given cooling rate was found to increase with the firing thermal budget. Increasing the temperature from 850 / 630 to 950 / 700°C had a larger effect than increasing the time from 1 to 11 h. The evolution of  $R_s$  upon annealing was also found to depend strongly on the cooling rate (furnace or quench). Although the magnitude of the effect varies for different pastes and firing temperatures and times, quenching always shifts the evolution of  $R_s$  to more negative values, in comparison with the corresponding furnace cooled sample.

DP 2041 ( $R_s$  change  $< 1.0\%$ ) was found to be the most stable paste. Even in this case, the observed changes (all positive) are larger than the full-scale piezoresistive response of corresponding sensors (around 0.3%). ESL 3414 shows similar behaviour, although with poorer stability (changes up to 8%). Except for the short standard firing cycle (10 min), the evolution tends to saturate, and even be partially reversed after ca. 200 h.

In spite of the much lower firing temperature of ESL 3114, its thermal stability is comparable to that of DP 2041. Samples made with slow furnace cooling exhibit low positive evolution of  $R_s$  upon annealing, which tends to saturate around  $+0.6\%$ . A similar negative evolution is observed for the sample fired under standard conditions. Quenched samples differ markedly, however, with  $R_s$  decreasing strongly upon annealing. In this case, increasing the firing thermal budget significantly improves stability.

At 250°C, possible evolution mechanisms could involve Ru in glass (dissolved or in clusters<sup>8</sup>), or mechanical relaxation. Our investigation methods did not allow direct assessment of Ru in glass, but local rearrangement of Ru in glass during annealing such as precipitation of supersaturated Ru into clusters cannot be ruled out.

Material	$R_s$ (kOhm)	$TCR$ (ppm/K)	$GF$ longitudinal	$GF$ transverse
DP 2041	11.0	58	11.6	8.1
ESL 3114	8.5	-243	10.7	8.7
ESL 3414	8.0	42	18.0	10.0

**Table 1. As-fired characteristics for the standard firing schedule.**

Changed parameter	DP 2041			ESL 3114			ESL 3414		
	$\Delta R_s$ (%)	$\Delta TCR$ (ppm/K)	$\Delta GF_1$ (%)	$\Delta R_s$ (%)	$\Delta TCR$ (ppm/K)	$\Delta GF_1$ (%)	$\Delta R_s$ (%)	$\Delta TCR$ (ppm/K)	$\Delta GF_1$ (%)
Increasing time	-43	+3	-13	-28	+26	-13	+39	-298	-12
Increasing temperature	-86	+18	-14	-45	+212	-36	/	/	/
Quenching	-3	-43	+2	-2	+45	+6	-40	-1	+6

**Table 2. Effect of firing parameters on as-fired characteristics.**

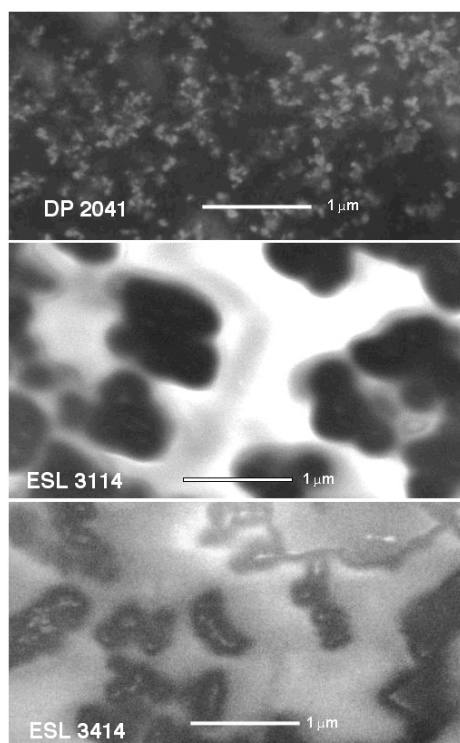


Figure 1. SEM of the surface of the resistors, standard firing conditions.

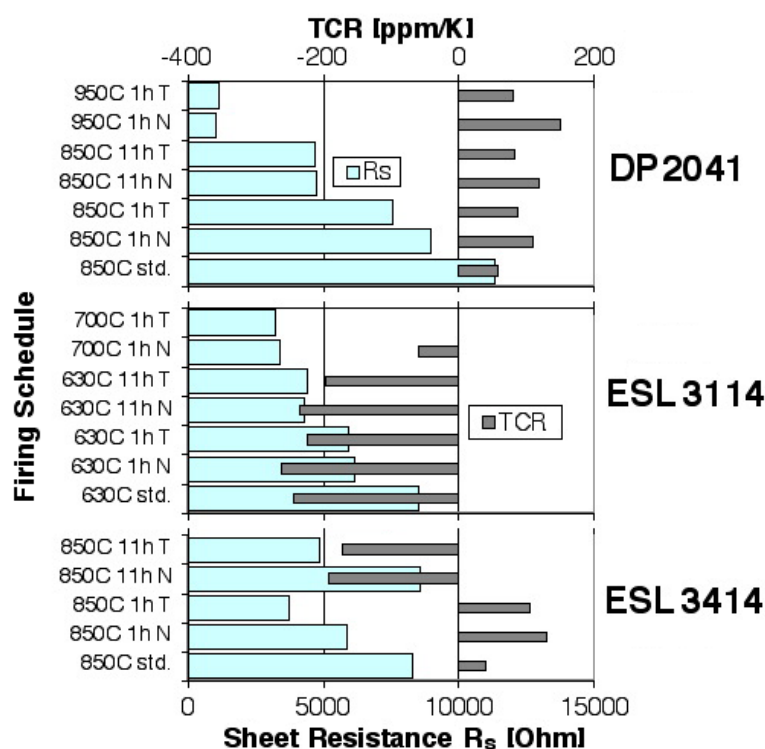


Figure 2. Initial values of sheet resistance  $R_s$  and temperature coefficient  $TCR$ . Std. = belt furnace; T = tube furnace, quenched; N = tube furnace, furnace cooled.

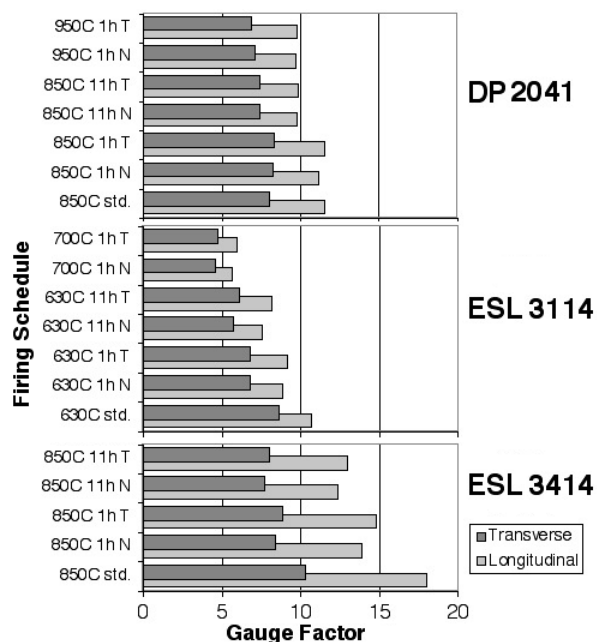


Figure 3. Initial gauge factors as a function of firing schedule. Std., T and N as in Fig.2.

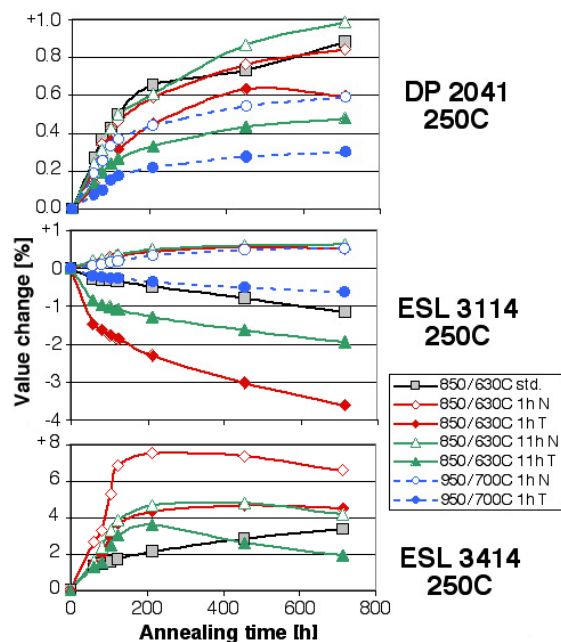


Figure 4. Relative change of sheet resistance  $R_s$  during the annealing.

Mechanical strain relaxation can be extrinsic (macroscopic thermal mismatch between resistor and substrate) or intrinsic (local thermal mismatch between glass and conductive phase). Extrinsic mismatch between Al<sub>2</sub>O<sub>3</sub> and standard 850°C firing resistors is thought to be small, as *TCE* values given for the glass<sup>11</sup> and RuO<sub>2</sub> (average<sup>12</sup>) are 7...8 and 5 ppm/K, close to the ca. 7 ppm/K value for Al<sub>2</sub>O<sub>3</sub>. However, the intrinsic, local thermal mismatches are much higher in the case of RuO<sub>2</sub>-containing resistors. Rutile RuO<sub>2</sub> has anisotropic *TCE* values: +9 and –2 ppm/K for the a=b and c axes. Upon quenching, strong tensile strains are therefore expected to be frozen in along the c axis, which can later relax during annealing. We could not verify whether a similar reasoning can be applied to Pb or Bi ruthenate containing resistors, as no *TCE* data was found for these compounds.

## 4 Conclusion

The influence of the firing schedule on the properties (*R<sub>s</sub>*, *GF* and *TCR*) was found to be different for the 3 tested compositions. Moreover, the changes of *R<sub>s</sub>*, *GF* and *TCR* are not intercorrelated. Upon annealing at 250°C, only *R<sub>s</sub>* changes significantly, and its stability was found to strongly depend on composition and firing schedule. ESL 3414 exhibited the highest changes, whereas DP 2041 and the low-firing ESL 3114 had comparable stability.

Increasing the cooling speed by quenching affects both properties and annealing behaviour. This could come from supersaturated Ru in the glass or from frozen-in local strains between conductive phase and glass matrix.

## References

- [1] Hrovat, M., Samardzija, Z., Holc, J., Belavić, D., Microstructural, XRD and electrical characterization of some thick film resistors. *Journal of Materials Science: Materials in Electronics*, 2000, **11**, 199-208.
- [2] Hrovat, M., Holc, J., Samardzija, Z., Belavić, D., The influence of firing temperature on gauge factors and the electrical and microstructural characteristics of thick film resistors. *J. of Materials Science Letters*, 2001, **20** (8), 701-705.
- [3] Hrovat, M., Samardzija, M., Belavic, D., Holc, J. & al, Microstructural and electrical characteristics of some “overfired” thick-film resistors. *Journal of Materials Science Letters*, 2001, **20** (4), 347-51.
- [4] Cattaneo, A., Marelli, M., Prudenziati, M., Effects of refiring processes on electrical and structural properties of thick-film resistors. In *Proceedings of the European Hybrid Microelectronics Conference*, 1979, **2**, 241-53.
- [5] Hrovat, M., Belavić, D., Samardzija, Z., Holc, J., The development of microstructural and electrical characteristics in some thick-film resistors during firing. *J. of Materials Science*, 2002, **37**, 2331-39.
- [6] Lee, J., Vest, R.W., Firing studies with a model thick film resistor system. In *IEEE Transactions on Components, Hybrids, and Manufacturing Technology*, dec. 1983, **CHMT-6**, n°4, 430-435.
- [7] Hrovat, M., Belavić, D., Samardzija, Z., Holc, J., The development of thick film resistor properties during firing. In *Conf. proceedings. MIDEEM, Soc. Microelectron. Components and Mater, Dunajaska, Slovenia*, 1999, 169-174.
- [8] Adachi, K., Iida, S., Hayashi, K., Ruthenium clusters in lead-borosilicate glass in thick film resistors. *Journal of Materials Research*, 1994, **9**, n°7, 1866-78.
- [9] Adachi, K., Kuno, H., Decomposition of ruthenium oxides in lead borosilicate glass. *Journal of the American Ceramic Society*, 1997, **80**, n°5, 1055-64.
- [10] Adachi, K., Kuno, H., Effect of glass composition on the electrical properties of thick-film resistors. *Journal of the American Ceramic Society*, 2000, **83**, n°10, 2441-48.
- [11] Trubnikov, L., Thermal expansion, vitrification temperature and corrosion behavior of lead-borosilicate glass, *Refractories and Industrial Ceramics*, 2000, **41**, 5/6, 169-171.
- [12] Krishna Rao, K.V., Iyengar, L., X-ray studies on the thermal expansion of ruthenium dioxide, *Acta Cryst.*, 1969, **A25**, 302.